Local-field effects and effective-medium theory: A microscopic perspective

D. E. Aspnes
Bell Laboratories, Murray Hill, New Jersey 07974

(Received 9 March 1981; accepted for publication 17 September 1981)

Standard textbook derivations of the Clausius–Mossotti (Lorentz–Lorenz) relation tend to obscure the physical origin of local-field effects by proceeding from the macroscopic dielectric function of the equivalent homogeneous system to the microscopic parameters of the model. The microscopic and macroscopic aspects can be made clearer by reversing the order, that is, by first obtaining the microscopic solution and then implementing the definition of macroscopic quantities as averages of their microscopic counterparts. This approach also leads naturally into a treatment of effective-medium theory and the description of the dielectric response of heterogeneous materials.

I. INTRODUCTION

The Clausius–Mossotti (Lorentz–Lorenz) relation is usually a student's only contact with local-field effects and the fundamental theory of the dielectric response of matter. The standard textbook derivation[1–5] begins by replacing the microscopic model, typically a simple cubic lattice of polarizable points, with a dielectrically equivalent homogeneous solid. An imaginary cavity is then used to introduce the concept of a local field and to express the microscopic polarizability of a lattice point as a function of the macroscopic observable, the dielectric function. This approach can hardly fail to be confusing to anyone wishing to master the physical principles involved, because both the cavity and the surface polarization charge on which the result depends are fictitious. Moreover, it is shown that the neighboring dipoles—precisely those that one would intuitively expect to contribute most strongly to a local field—apparently contribute nothing. Further problems arise if one attempts to apply the formalism to low-symmetry configurations such as linear molecules, for which a spherical cavity may not be appropriate,[6,7] or to dipoles on a surface, for which the spherical cavity has no obvious analog.

The confusion arises for a simple reason. In electrodynamics, as in thermodynamics, the length scales of laboratory probes are usually far larger than those that describe a system on the microscopic (typically atomic) level where interactions are actually taking place. Therefore, laboratory probes measure averages of microscopic responses. Consequently, the description or derivation of a macroscopic quantity such as the dielectric function in terms of the actual microscopic parameters must involve two distinct steps. One consists of solving the microscopic problem exactly, and the other consists of taking suitable averages of the microscopic solution to calculate the macroscopic observables.[8]

Thermodynamicists long ago recognized the futility of trying to implement the first half of this prescription for random macroscopic systems, because such an approach would necessarily involve enormous numbers of equations, e.g., six for each molecule of a gas. They rather concentrated on the second half, by first defining macroscopic average or observable quantities such as pressure, temperature, or entropy, and then establishing dependences among them, such as $PV = nRT$. Maxwell's equations are completely analogous in that they also express dependences among macroscopic average or observable quantities, in this case the electromagnetic fields **E**, **D**, **H**, and **B**.[9] Here, the microscopic reaction of a physical system to an external field is represented entirely (and phenomenologically) by dielectric functions ϵ and magnetic permeabilities μ, which enter through the constitutive relations $\mathbf{D} = \epsilon\mathbf{E}$ and $\mathbf{B} = \mu\mathbf{H}$. For electrodynamic purposes this approach is entirely adequate. But if one wishes to understand the origin of dielectric response functions, or needs to deal with the dielectric properties of heterogeneous materials such as glasses, amorphous and polycrystalline semiconductors, and metal films, or two-dimensional arrays such as molecules adsorbed on a surface, then the microscopic aspects cannot be ignored.

The standard textbook treatment of the simple cubic lattice of point dipoles as an idealized model of the local-field problem is a classic example of the thermodynamic approach of emphasizing the macroscopic average. One begins with the dielectric function of the equivalent homogeneous solid and solves only enough of the microscopic problem to establish the connection of ϵ to the polarizability of its microscopic constituents. In this paper we show that the alternative approach, where one implements the basic definition of macroscopic quantities as suitable averages of their microscopic counterparts, yields a physically more meaningful derivation of the Clausius–Mossotti relation, one in which the definition of the local field, the role of induced internal dipole fields, and the connection between macroscopic average and microscopic fields are all clearly defined. Although both approaches can be shown to be equivalent,[8] the microscopic treatment leads naturally into discussions of more elaborate models. These models incorporate intermolecular interactions and other higher-order corrections, and are used to describe the dielectric response of a wide variety of physical systems of current interest ranging from solar-absorbing three-dimensional composites to monolayers adsorbed on clean surfaces.

II. AVERAGE/SOLVE: THE MACROSCOPIC APPROACH

We review briefly the standard treatment based on a spherical cavity; more complete details can be found elsewhere.[2] We suppose that the points of polarizability α are arrayed at sites $\mathbf{r} = \mathbf{R}_i$ of a simple cubic lattice centered at the coordinate origin, as indicated schematically in Fig. 1. If the material is first considered spatially homogeneous with a dielectric function ϵ, then a uniform applied field **E**

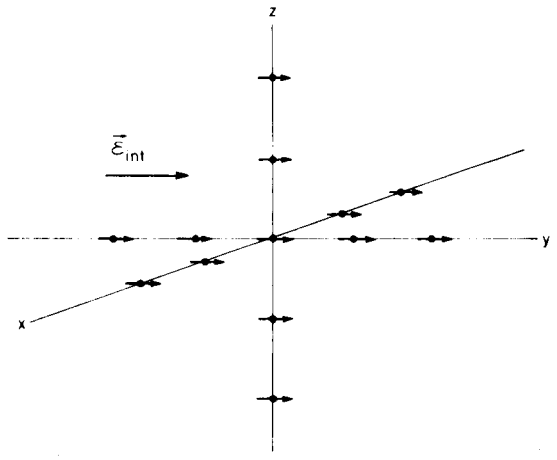

Fig. 1. Schematic diagram of the simple cubic lattice used in the derivation of the Clausius–Mossotti relation. $\mathbf{E}_{int}$ is a uniform applied field.

will generate a uniform dipole moment per unit volume, **P**, where **P** and **E** are related to **D** and ϵ by the macroscopic definitions

$$\mathbf{D} = \epsilon\mathbf{E}, \tag{1a}$$

$$= \mathbf{E} + 4\pi\mathbf{P}. \tag{1b}$$

We wish to relate the polarizability α of the dipole at the coordinate origin to ϵ. Clearly, the discrete nature of the lattice must be taken into account at the origin and probably also for a range of neighboring dipoles about the origin, even though at sufficiently large distances the homogeneous approximation can be considered valid. Accordingly, we divide the lattice into homogeneous (macroscopic) and discrete (microscopic) phases at a fictitious spherical boundary $r_0 \gg a$, where a is the lattice constant, as shown in Fig. 2. The field $\mathbf{E}_{loc}$ at the dipole at the center of the fictitious cavity will therefore be **E** plus the contribution from the polarization of the uniform region outside the boundary (represented by **P**) plus the contributions from the neighboring dipoles within the cavity. Because **P** is uniform over the region outside the cavity, the polarization

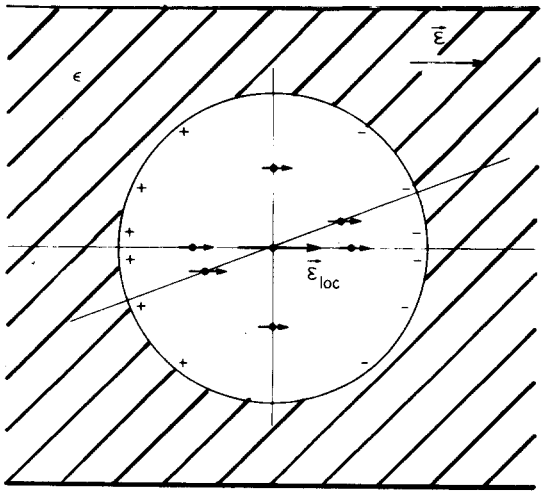

Fig. 2. As Fig. 1, but showing a spherical boundary separating the lattice into homogeneous (macroscopic) and discrete (microscopic) phases. $\mathbf{E}_{loc}$ is the field at the center of the cavity.

charge density $\nabla\cdot\mathbf{P}$ is zero everywhere except at the cavity boundary where the discontinuity gives rise to a surface charge density $\sigma = -\mathbf{P}\cdot\hat{n}$, where $\hat{n}$ is the outward normal unit vector. The integral over the boundary charge can be done explicitly[2] and we have

$$\mathbf{E}_{loc} = \mathbf{E} + \frac{4\pi}{3}\mathbf{P} + \sum_i \mathbf{E}(\mathbf{p}, -\mathbf{R}_i), \tag{2}$$

where $\mathbf{E}(\mathbf{p}, \mathbf{r})$ is the electric field at **r** of a dipole **p** located at the origin:

$$\mathbf{E}(\mathbf{p}, \mathbf{r}) = -\nabla\left(\frac{\mathbf{p}\cdot\hat{r}}{r^2}\right) \tag{3a}$$

$$= \frac{3(\mathbf{p}\cdot\hat{r})\hat{r} - \mathbf{p}}{r^3}. \tag{3b}$$

The sum in Eq. (2) is restricted to those $\mathbf{R}_i$ within the cavity.

It is easy to show by evaluating the sum explicitly that the contributions from all dipoles on a given shell $|\mathbf{R}_i|$ cancel identically for the simple cubic lattice. Then Eq. (2) reduces to the well-known result

$$\mathbf{E}_{loc} = \mathbf{E} + (4\pi/3)\mathbf{P}. \tag{4}$$

If the polarizability of each point is α, the dipole moment of the central point, and by symmetry that of all points, is therefore

$$\mathbf{p} = \alpha\mathbf{E}_{loc}. \tag{5}$$

Then the dipole moment per unit volume within the cavity, equal of course to that outside the cavity, can be calculated from the definitions

$$\mathbf{P} = \frac{1}{V}\int_V d^3r\, \mathbf{r}\,\rho(\mathbf{r}), \tag{6a}$$

$$= \frac{1}{V}\int_V d^3r\, \mathbf{p}(\mathbf{r}) \tag{6b}$$

$$= \frac{1}{V}\sum_i \mathbf{p}_i, \tag{6c}$$

where $\rho(\mathbf{r})$ is the charge density and V is the volume of the system. Equations (6b) and (6c) apply to distributed and discrete dipoles $\mathbf{p}(\mathbf{r})$ and $\mathbf{p}_i$, respectively. We find from Eq. (6c) that

$$\mathbf{P} = n\mathbf{p} = n\alpha\mathbf{E}_{loc}, \tag{7}$$

where $n = a^{-3}$ is the number of points per unit volume. If Eq. (7) is first used to eliminate **P** from Eqs. (1) and (4), and Eq. (4) is then used to eliminate $\mathbf{E}_{loc}$ from Eq. (1), then α can be written in terms of ϵ as

$$\frac{4\pi}{3}n\alpha = \frac{\epsilon - 1}{\epsilon + 2}. \tag{8}$$

This is the Clausius–Mossotti result.

III. SOLVE/AVERAGE: THE MICROSCOPIC PERSPECTIVE

We consider the same configuration but begin with the premise that the microscopic lattice structure extends to infinity, as shown in Fig. 1. Let a uniform field $\mathbf{E}_{int}$, as yet unspecified, be applied. $\mathbf{E}_{int}$ will induce a dipole $\mathbf{p}_i = \alpha\mathbf{E}(\mathbf{R}_i)$ at each site $\mathbf{R}_i$ according to the value of the field $\mathbf{E}(\mathbf{R}_i)$ at $\mathbf{R}_i$. Again, symmetry insures that all $\mathbf{E}(\mathbf{R}_i) = \mathbf{E}_{loc}$ are equal for the simple cubic lattice.

We require first the microscopic solution, that is, expres-

sions for the field $\mathbf{E}(\mathbf{r})$ and dipole distribution $\mathbf{p}(\mathbf{r})$ that are valid at every point in space. $\mathbf{E}(\mathbf{r})$ clearly has the form

$$\mathbf{E}(\mathbf{r}) = \mathbf{E}_{\text{int}} + \sum_i \mathbf{E}(\mathbf{p}_i, \mathbf{r} - \mathbf{R}_i), \tag{9}$$

where $\mathbf{E}(\mathbf{p}, \mathbf{r})$ is given by Eq. (3) and the sum now extends over all $\mathbf{R}_i$. Similarly, $\mathbf{p}(\mathbf{r})$ must have the form

$$\mathbf{p}(\mathbf{r}) = \sum_i \alpha \mathbf{E}(\mathbf{R}_i)\delta(\mathbf{r} - \mathbf{R}_i), \tag{10}$$

since the dipoles are located only at lattice sites.

Equation (9) is general, so it must also apply to lattice sites $\mathbf{R}_i$. For $\mathbf{r} = 0$, we have

$$\mathbf{E}_{\text{loc}} = \mathbf{E}(0) = \mathbf{E}_{\text{int}} + {\sum_i}' \mathbf{E}(\alpha \mathbf{E}_{\text{loc}}, -\mathbf{R}_i) \tag{11a}$$

$$= \mathbf{E}_{\text{int}}. \tag{11b}$$

The prime on the summation means that we exclude the singular term that results for $\mathbf{R} = 0$. Equation (11b) follows because the summation vanishes shell by shell for the simple cubic lattice. The microscopic problem has now been solved, because $\mathbf{p}(\mathbf{r})$ and $\mathbf{E}(\mathbf{r})$ are given for all $\mathbf{r}$ in terms of the microscopic parameters and $\mathbf{E}_{\text{int}}$:

$$\mathbf{E}(\mathbf{r}) = \mathbf{E}_{\text{loc}} + \sum_i \mathbf{E}(\alpha \mathbf{E}_{\text{loc}}, \mathbf{r} - \mathbf{R}_i), \tag{12a}$$

$$\mathbf{p}(\mathbf{r}) = \sum_i \alpha \mathbf{E}_{\text{loc}} \delta(\mathbf{r} - \mathbf{R}_i), \tag{12b}$$

$$\mathbf{E}_{\text{loc}} = \mathbf{E}_{\text{int}}. \tag{12c}$$

The second step is to implement the basic definition of a macroscopic quantity[1,10] and volume average $\mathbf{E}(\mathbf{r})$ and $\mathbf{p}(\mathbf{r})$ to obtain the corresponding macroscopic parameters $\mathbf{E}$ and $\mathbf{P}$ used in Eq. (1). We find from Eqs. (6b) and (12b) that

$$\mathbf{P} = n\alpha \mathbf{E}_{\text{loc}}, \tag{13}$$

which is identical to Eq. (7). To calculate the volume average of Eq. (12a) we need first to evaluate the volume integral of $\mathbf{E}(\mathbf{p}, \mathbf{r})$ over a region containing $\mathbf{p}$:

$$\int_{\text{vol}} d^3r\, \mathbf{E}(\mathbf{p}, \mathbf{r}) = -\int_{\text{vol}} d^3r\, \nabla\left(\frac{\mathbf{p}\cdot\hat{r}}{r^2}\right) \tag{14a}$$

$$= -\int_{\text{surf}} d^2r \left(\frac{\mathbf{p}\cdot\hat{r}}{r^2}\right)\hat{n} \tag{14b}$$

$$= -(4\pi/3)\mathbf{p}. \tag{14c}$$

With this result we have

$$\mathbf{E} = \mathbf{E}_{\text{loc}} - (4\pi/3)n\alpha \mathbf{E}_{\text{loc}} \tag{15a}$$

$$= \mathbf{E}_{\text{loc}} - (4\pi/3)\mathbf{P} \tag{15b}$$

by Eqs. (10) and (11b). Equation (15b) is identical to Eq. (4), except for the fact that the term involving $\mathbf{P}$ appears on the other side. Consequently, the Clausius–Mossotti relation follows as in Sec. II.

Two points of the microscopic approach are worth noting, as they clarify confusing aspects of the macroscopic derivation. First, the microscopic uniform internal field $\mathbf{E}_{\text{int}}$ that is actually applied is larger than the macroscopic uniform field $\mathbf{E}$ that is apparently applied because $\mathbf{E}_{\text{int}}$ is opposed on the average by the fields of the induced dipoles, as shown by Eq. (15b). The average opposition field is generated on a dipole-by-dipole basis. The dominant contribution from a given dipole occurs in the vicinity of the dipole because dipole fields fall off rapidly with increasing distance [see Eq. (3b)]. Implications that contributions from dipoles in remote regions are important, as suggested by the cavity derivation, are not correct. The role of the cavity is simply to simulate the fact that the volume integral of the dipole field is not zero but $-(4\pi/3)\mathbf{p}$. A more accurate interpretation of the source of the fictitious boundary charge is that it arises from the (also macroscopically homogeneous) *interior* region of the cavity. Thus the apparent failure of the neighboring dipoles to contribute to the local field in the cavity model occurs because their contributions are already implicitly contained in the fictitious boundary charge.

Second, Eq. (11a) is a self-consistent relation for $\mathbf{E}_{\text{loc}}$. In low-symmetry configurations, the summation term usually does not vanish and the constant of proportionality between $\mathbf{E}_{\text{loc}}$ and $\mathbf{E}_{\text{int}}$ is greater or less than unity depending on whether the fields from the adjacent dipoles add to or subtract from the applied field $\mathbf{E}_{\text{int}}$. For example, for a two-dimensional square array of point dipoles of polarizability α and lattice constant a, Eq. (11a) reduces to[11]

$$\mathbf{E}_{\text{loc}} = \mathbf{E}_{\text{int}} + 4.517(\alpha/a^3)\mathbf{E}_{\text{loc}} \quad \mathbf{E}\parallel \text{plane}, \tag{16a}$$

$$= \mathbf{E}_{\text{int}} - 9.034(\alpha/a^3)\mathbf{E}_{\text{loc}} \quad \mathbf{E}\perp \text{plane}. \tag{16b}$$

For this case the result is polarization dependent: the dipole fields add to the applied field if the field is oriented parallel to the two-dimensional array, and oppose it if the field is oriented perpendicular to the array. Other proportionality constants are obtained for hexagonal arrays or for image-charge effects.[11] These effects are important in calculating the dielectric response of adsorbed monolayers[12] and in some models of surface-enhanced Raman scattering.[13] This aspect of the local-field problem leads to conditions on the on- and off-diagonal components of the full dielectric tensor when the atomic microstructure is considered for real materials.[14]

IV. HETEROGENEOUS DIELECTRICS AND EFFECTIVE-MEDIUM THEORY

The microscopic approach is ideally suited for treating heterogeneous materials, which are mixtures of constituents of different polarizabilities. As a simple example we can assign different polarizabilities, α_a and α_b, at random to the points of the cubic lattice. Equations (9) and (10) clearly retain their same form. If we suppose that the summation term in Eq. (11a) still cancels so that $\mathbf{E}_{\text{loc}} = \mathbf{E}_{\text{int}}$ as before, the volume averages now yield

$$\mathbf{P} = (n_a\alpha_a + n_b\alpha_b)\mathbf{E}_{\text{loc}}, \tag{17a}$$

$$\mathbf{E} = \mathbf{E}_{\text{loc}} - (4\pi/3)\mathbf{P}, \tag{17b}$$

where n_a and n_b are the volume densities of points a and b. The dielectric function of the mixture can be calculated from Eq. (1) as before and we find

$$\frac{\epsilon - 1}{\epsilon + 2} = \frac{4\pi}{3}(n_a\alpha_a + n_B\alpha_b). \tag{18}$$

It is convenient to rewrite Eq. (18) in terms of the dielectric functions ϵ_a and ϵ_b of the pure phases a and b by means of Eq. (8). Then

$$\frac{\epsilon - 1}{\epsilon + 2} = f_a\frac{\epsilon_a - 1}{\epsilon_a + 2} + f_b\frac{\epsilon_b - 1}{\epsilon_b + 2}, \tag{19}$$

where f_i represents the volume fraction of the ith phase:

$$f_i = n_i / \left(\sum_j n_j \right), \quad \sum_i f_i = 1. \tag{20}$$

Equation (19) is the Lorentz-Lorenz effective-medium expression.[1,15] It can obviously be generalized to systems containing more than two phases by adding more terms. Another generalization is to include intermolecular interactions to more accurately describe dense mixtures.[16] Numerous generalizations of a more phenomenological nature have been recently reviewed by Grosse and Greffe.[17]

More usually, heterogeneous materials consist of microscopic regions small compared to the wavelength of light but still large enough to possess their own dielectric identity. In this case the previous derivation must be modified even though the solve–average approach remains valid. For example, suppose a spherical inclusion of dielectric function ϵ_a and radius r_a is embedded in a medium of dielectric function ϵ_b. The microscopic solution for an applied field $\mathbf{E}_0$ uniform at large distances is[10]

$$\mathbf{E}(\mathbf{r}) = \frac{3\epsilon_b}{\epsilon_a + 2\epsilon_b} \mathbf{E}_0 \quad |\mathbf{r}| < r_a, \tag{21a}$$

$$\mathbf{E}_0 + \mathbf{E}(\mathbf{p}_a, \mathbf{r}) \quad |\mathbf{r}| > r_a, \tag{21b}$$

where $\mathbf{E}(\mathbf{p}, \mathbf{r})$ is defined by Eq. (3) and

$$\mathbf{p}_a = \frac{\epsilon_a - \epsilon_b}{\epsilon_a + 2\epsilon_b} r_a^3 \mathbf{E}_0. \tag{21c}$$

The microscopic expression for the dipole moment per unit volume follows from Eq. (1):

$$\mathbf{P}_i(\mathbf{r}) = \frac{\epsilon_i - 1}{4\pi} \mathbf{E}(\mathbf{r}), \tag{22}$$

where $\epsilon_i = \epsilon_a$ or ϵ_b according to whether $\mathbf{r}$ is located in region a or region b. Performing the volume averages and using Eq. (1) to calculate ϵ in terms of the macroscopic parameters $\mathbf{E}$ and $\mathbf{P}$ yields

$$\frac{\epsilon - \epsilon_b}{\epsilon + 2\epsilon_b} = f_a \frac{\epsilon_a - \epsilon_b}{\epsilon_a + 2\epsilon_b}, \tag{23a}$$

where

$$f_a = (4\pi/3) r_a^3 / V \tag{23b}$$

is the volume fraction occupied by the phase a and V is the total volume of the system. Equation (23a) is the Maxwell Garnett effective-medium expression.[18]

Equations (19) and (23a) have the same general form

$$\frac{\epsilon - \epsilon_h}{\epsilon + 2\epsilon_h} = f_a \frac{\epsilon_a - \epsilon_h}{\epsilon_a + 2\epsilon_h} + f_b \frac{\epsilon_b - \epsilon_h}{\epsilon_b + 2\epsilon_h}, \tag{24}$$

where ϵ_h is the dielectric function of a host medium. Thus ϵ_h equals 1 (void) and ϵ_b for the Lorentz–Lorenz and Maxwell Garnett expressions, respectively. If $f_a > f_b$, then a more appropriate choice for ϵ_h in the Maxwell Garnett case is ϵ_a. However, the resulting values of ϵ are different for the two choices. Bruggeman[19] resolved this dilemma by proposing that neither phase should be given preference, but that the inclusions should be considered as being embedded in the effective medium itself. In the above formulation this is equivalent to choosing $\epsilon_h = \epsilon$, in which case the left-hand side of Eq. (24) vanishes and

$$0 = f_a \frac{\epsilon_a - \epsilon}{\epsilon_a + 2\epsilon} + f_b \frac{\epsilon_b - \epsilon}{\epsilon_b + 2\epsilon}. \tag{25}$$

This is the Bruggeman effective-medium expression, or in conventional terminology, the *effective-medium approximation* (EMA). Although Eqs. (19), (23a), and (25) are superficially quite different, the above discussion shows that they are all related and differ only in the choice of the host dielectric ϵ_h.[20] The generalizations to mixtures of more than two dielectrics is obvious.

The Maxwell Garnett and Bruggeman expressions have been derived many different ways, generally by requiring that the scattering of a wave off an inclusion shall vanish in the forward direction.[18,19,21,22] Recent treatments[21,22] have attempted to understand their differences more fundamentally in terms of the microstructure of the composite material. These investigations showed that the Maxwell Garnett result follows from a coated-sphere (cermet) configuration, where inclusions of phase a are completely surrounded by material of phase b. The Bruggeman expression follows from an aggregate model, where particles of phase a and phase b are mixed on a random basis. These conclusions are, of course, completely consistent with the corresponding choices of host material, ϵ_h, in the derivations of Eqs. (23a) and (25).

We comment finally on the importance of microstructure in effective medium theories. The average microstructure has obviously entered Eq. (24) through the volume fractions f_a and f_b. But the detailed microstructure has also entered implicity through the assumptions that the inclusions were spherical and noninteracting. These assumptions are hardly ever satisfied in actual heterogeneous materials, which generally have a random and complex form. The shape of the particles determines how effectively they are screened, which affects the microscopic polarizations and fields, which in turn determines the functional relationship between ϵ and the dielectric functions of the constituents.

The role of screening can be understood by considering a small metal sphere embedded in an insulator as indicated schematically in Fig. 3. If an electric field is applied, the high conductivity of the metal insures that a screening charge will develop at its boundary. To lowest order the field will be completely screened out of the sphere, which consequently will not be "seen" by the external field. If one neglects the screening effect and naively calculates ϵ by averaging the dielectric functions of host and sphere weighted according to volume fraction, then the contribution of the sphere to ϵ will clearly be overestimated. In general, the more polarizable fractions contribute less than expected on the basis of simple volume averages because they develop more polarization charge and are screened

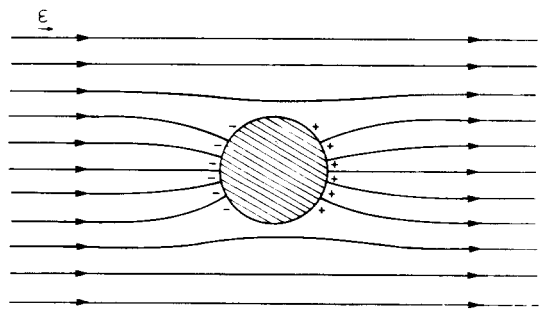

Fig. 3. Screening of a small metal sphere in a dielectric medium under an applied field.

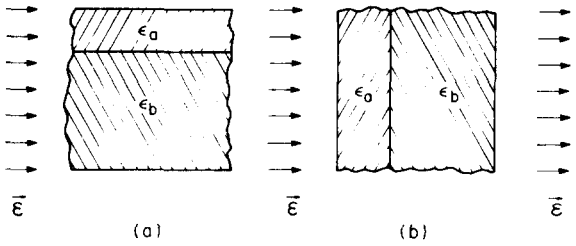

Fig. 4. Limiting cases of a microstructure with (a) no screening; (b) maximum screening.

more effectively. Likewise, a needle-shaped inclusion oriented parallel to the field will develop little screening charge and will contribute more to ϵ than a disc-shaped inclusion of the same volume oriented perpendicular to the field. Expressions analogous to Eqs. (19), (23a), and (25) giving ϵ for elliptical and more generally shaped inclusions have been discussed by Granqvist and Hunderi.[23]

The two limiting cases representing no screening and maximum screening are shown in Figs. 4(a) and 4(b), respectively. In the former case the field $\mathbf{E}(\mathbf{r}) = \mathbf{E}$ is uniform over the composite, and $\mathbf{P}(\mathbf{r}) = [(\epsilon_i - 1)/4\pi]\mathbf{E}$, where $\epsilon_i = \epsilon_a$ or ϵ_b according to whether $\mathbf{r}$ is located in region a or b, respectively. Averaging these expressions and using Eq. (1) yields

$$\epsilon_{\parallel} = f_a\epsilon_a + f_b\epsilon_b, \tag{26}$$

Thus if no screening occurs, a simple volume average results. For maximum screening $\mathbf{D}$ is uniform over the composite and a similar calculation yields

$$\epsilon_{\perp} = (f_a/\epsilon_a + f_b/\epsilon_b)^{-1}. \tag{27}$$

Equations (26) and (27) are equivalent in form to those describing conductances or capacitances connected in parallel and in series, respectively. In this sense effective-medium theory provides a circuit diagram for the composite material.

Because there can never be less screening than no screening (all boundaries parallel to the applied field) nor more screening than maximum screening (all boundaries perpendicular to the applied field), one may guess from the above discussion that the allowed range of ϵ is not arbitrary but has well-defined limits. In fact, Eqs. (26) and (27) define the absolute Wiener bounds[24] to ϵ for a two-phase composite regardless of composition or microstructure. Much recent effort has been devoted to establishing more stringent limits based on very general macroscopic attributes such as composition[25] and two- or three-dimensional isotropy.[26,27] The results can be summarized simply in terms of the limiting cases above. We suppose that the dielectric functions ϵ_a and ϵ_b of the constituents a and b are known, and locate these values on the complex ϵ plane as shown in Fig. 5.[27] In this example, $\epsilon_a = -2 + i3$ and $\epsilon_b = 1 + i1$. If nothing else is known, the effective dielectric function for any composition and microstructure must lie within the absolute Wiener bounds given by the straight line connecting ϵ_a and ϵ_b [Eq. (26)] and the circular arc passing through the points ϵ_a, ϵ_b, and 0 [Eq. (27)]. If the compositions f_a and f_b are known, then ϵ must lie within the smaller region defined by the circular arcs passing through the appropriate points $\epsilon_{\parallel}$ and $\epsilon_{\perp}$ on the absolute Wiener bounds and either ϵ_a or ϵ_b.[25] It can be shown that the Maxwell Garnett values ϵ_{MGa} and ϵ_{MGb} obtained by taking $\epsilon_h = \epsilon_a$ and $\epsilon_h = \epsilon_b$, respectively,

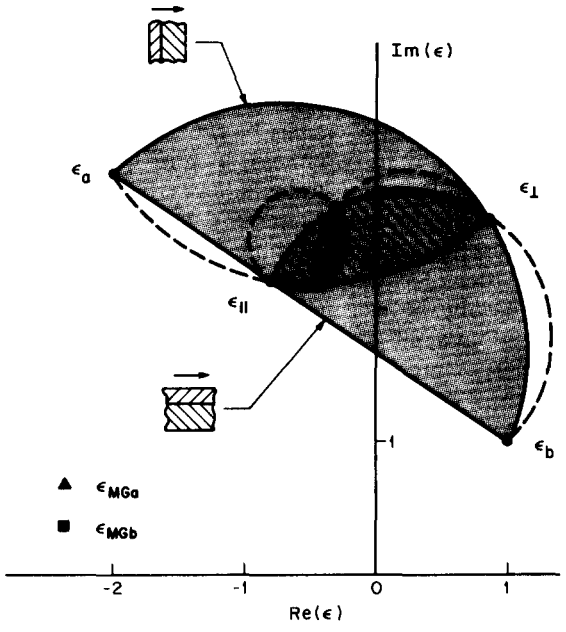

Fig. 5. Allowed values of ϵ for a two-component heterogeneous dielectric. The largest region defines the allowed range of ϵ if no information on composition or microstructure is available. The next region illustrates the allowed range if the composition (here 60% a, 40% b) is known. The smallest region applies if the composite is macroscopically isotropic (after Ref. 27).

in Eq. (24) also lie on these arcs. Finally, if the composite is known to be macroscopically isotropic, then the dielectric function must lie within the much smaller region defined by the circular arcs passing through ϵ_{MGa} and ϵ_{MGb} and either $\epsilon_{\parallel}$ or $\epsilon_{\perp}$, as shown.[26,27] Thus rather general assumptions can lead to fairly tight constraints on allowed values of ϵ regardless of the actual details of the microstructure.[24–27]

[1]H. A. Lorentz, *Theory of Electrons*, 2nd ed. (Teubner, Leipzig, 1916), Chap. 4.

[2]J. D. Jackson, *Classical Electrodynamics* (Wiley, New York, 1962), Sec. 4.6.

[3]R. P. Feynman, R. B. Leighton, and M. Sands, *The Feynman Lectures on Physics, Vol. 2* (Addison-Wesley, Reading, MA, 1964), Sec. 11.

[4]M. Born and E. Wolf, *Principles of Optics*, 5th ed. (Pergamon, New York, 1975), Chap. 2.

[5]C. Kittel, *Introduction to Solid State Physics*, 5th ed. (Wiley, New York, 1976), Chap. 13.

[6]C. J. F. Bottcher, *Theory of Electric Polarization* (Elsevier, New York, 1952).

[7]R. Landauer, in *Proceedings of the First Conference on the Electrical Transport and Optical Properties of Inhomogeneous Media*, edited by J. C. Garland and D. B. Tanner, AIP Conf. Proc. No. 40 (AIP, New York, 1978), p.2.

[8]J. van Kranendonk and J. E. Sipe, in *Progress in Optics, Vol. 15*, edited by E. Wolf (North-Holland, Amsterdam, 1977), p. 245.

[9]It is worth noting that Maxwell had already achieved considerable stature in the field of thermodynamics before starting his work on the description of electromagnetic phenomena. The four "Maxwell's equations" to a thermodynamicist are not $\nabla\cdot\mathbf{B} = 0$, etc., but rather $(\partial T/\partial V)_S = -(\partial P/\partial S)_V$, etc. See, e.g., M. W. Zemansky, *Heat and Thermodynamics* (McGraw-Hill, New York, 1957), p. 244.

[10]Jackson, Ref. 2, Sec. 4.4.

[11]J. Topping, Proc. R. Soc. London A **114**, 67 (1927): M. J. Dignam and M. Moskovitz, J. Chem. Soc., Faraday Trans. 2, **69**, 56 (1973).

[12]F. H. P. M. Habraken, O. L. J. Gijzeman, and G. A. Bootsma, Surf. Sci. **96**, 482 (1980).
[13]T. E. Furtak and J. Reyes, Surf. Sci. **93**, 351 (1980).
[14]S. L. Adler, Phys. Rev. **126**, 413 (1962); N. Wiser, Phys. Rev. **129**, 62 (1963).
[15]L. Lorenz, Ann. Phys. Chem. (Leipzig) **11**, 70 (1880).
[16]M. Omini, Physica (Utrecht) **83A**, 431 (1976); **84**, 129, 492 (1976); K. Vedam and P. Limsuwan, J. Chem. Phys. **69**, 4772 (1978).
[17]C. Grosse and J. L. Greffe, J. Chim. Phys. **76**, 305 (1979).
[18]J. C. M. Garnett, Philos. Trans. R. Soc. London **203**, 385 (1904); A **205**, 237 (1906).
[19]D. A. G. Bruggeman, Ann. Phys. (Leipzig) **24**, 636 (1935).
[20]D. E. Aspnes, J. B. Theeten, and F. Hottier, Phys. Rev. B **20**, 3292 (1979).
[21]G. B. Smith, J. Phys. D **10**, L39 (1977).
[22]G. A. Niklasson, C. G. Granqvist, and O. Hunderi, Appl. Opt. **20**, 26 (1981).
[23]C. G. Granqvist and O. Hunderi, Phys. Rev. B **18**, 2897 (1978).
[24]O. Wiener, Abh. Math. Phys. K1. Königl. Sächs. Ges. **32**, 509 (1912).
[25]Z. Hashin and S. Shtrikman, J. Appl. Phys. **33**, 3125 (1962).
[26]D. Bergmann, Phys. Rev. Lett. **44**, 1285 (1980).
[27]D. W. Milton, Appl. Phys. Lett. **37**, 300 (1980).

Nuclear spins in the Earth's magnetic field

P. T. Callaghan and M. Le Gros
Department of Chemistry, Biochemistry and Biophysics, Massey University, Palmerston North, New Zealand

(Received 24 March 1981; accepted for publication 11 November 1981)

Details are given of a simple apparatus for the observation of nuclear precession in the Earth's magnetic field. Spin echos are generated using a pulse of oscillatory magnetic field resonant at the Larmor frequency. Students can use the system to measure a nuclear magnetic moment, nuclear relaxation times, and the local strength and orientation of the Earth's magnetic field.

INTRODUCTION

The study of nuclear magnetism is one of those areas of physics which seems to endure beyond all expectations. Indeed few techniques have yielded so rich a harvest in physics, chemistry, and biology as the observations of nuclear spin dynamics. Nuclear spin manipulation is even responsible for the lowest laboratory temperature to date! This remarkable versatility of application results from the wide range of magnitudes manifest in the interaction of nuclear spin and environmental electromagnetic properties. An appreciation of nuclear magnetism is well within the grasp of an undergraduate physics student and an inexpensive apparatus which illustrates some of the fundamentals of the subject can be easily constructed. We describe here some simple equipment which can be used as the basis for a nuclear magnetism experiment in the teaching laboratory. Variations of this technique have been used in geomagnetic field measurements for many years but in our experiment the student not only measures precisely the magnitude of the Earth's local magnetic field but can also obtain the nuclear dipole moment of ^{19}F and the relaxation times of either ^{1}H and ^{19}F nuclei in different chemical environments. A novel aspect of our system is that it enables the observation of spin echos in the Earth's magnetic field. The spin echo is generated by a pulse of magnetic field oscillating at the Larmor frequency and is an audio frequency analog of the 180° rf pulse used in the traditional NMR spin echo sequence.

DETECTING NUCLEAR MAGNETISM

Whenever the polarization axis of a nuclear dipole ensemble is momentarily displaced from the polarizing magnetic field direction an oscillatory emf can be subsequently detected in a receiver coil oriented perpendicular to the field.[1] This decaying emf, known as the free induction decay (FID), results from the Larmor precession about the static magnetic field of the nuclear spin angular momentum vectors. The decay rate is governed by the nuclear spin–spin interaction which cause a relentless loss of phase coherence in the nuclear ensemble. For an ensemble of similar spin-$\frac{1}{2}$ nuclei, the FID signal is accurately described by[2]

$$S(t) = S_0 \exp(-t/T_2)\cos(\gamma B_0 t + \alpha), \tag{1}$$

where T_2 is the transverse or spin–spin relaxation time and γB_0 is the Larmor precession frequency, proportional both to the static environmental magnetic field B_0 and to the nuclear gyromagnetic ratio γ. γ is a constant relating the nuclear magnetic dipole moment μ to the spin angular momentum quantum number j via the equation

$$\mu = \gamma \hbar j. \tag{2}$$

Where the static magnetic field in which the nuclei are to precess is the local field of the Earth, a simple means of reorienting the nuclear spin magnetization is to momentarily apply a much larger laboratory magnetic field in a transverse direction. This method was first suggested by Packard and Varian[3] who demonstrated that a simple but precise magnetometer could be constructed using the coil configuration shown in Fig. 1 with a water sample abundant in ^{1}H spins. The transverse polarizing field B_p, if applied for longer than a few spin-lattice relaxation times T_1, induces a larger transverse proton magnetization which subsequently precesses about the Earth's magnetic field on removing the polarizing field. B_p thus had a dual purpose